A MULTITEXTURE MODEL FOR MULTILOOK POLARIMETRIC RADAR DATA

Torbjørn Eltoft, Stian Normann Anfinsen, and Anthony Paul Doulgeris

University of Tromsø, Department of Physics and Technology, NO-9037 Tromsø, Norway

ABSTRACT

A statistical model for multilook polarimetric radar data is presented where the polarimetric channels are associated with individual texture variables having potentially different statistical properties. The feasibility of producing closed form probability density functions under certain restrictions is outlined. Mellin kind statistics are derived under various assumptions on the texture variables, and the potential for model fit assessment and hypothesis testing in the Mellin domain is demonstrated. Application to real data proves the usefulness of the analytic approach.

Index Terms— Radar polarimetry, synthetic aperture radar, probability density functions, texture modeling

1. INTRODUCTION

Knowledge of the exact statistical properties of polarimetric synthetic aperture radar (SAR) data forms the basis for image analysis techniques such as segmentation and land cover classification (e.g. [1]). In the literature, Gaussian signal statistics is often taken as the default hypothesis. Analysis of real SAR images reveals that non-Gaussian models give better representation of the data, implying that processing algorithms based on such models should improve performance.

The multivariate product model has been widely used in non-Gaussian modeling, processing, and analysis of polarimetric SAR images [1,2]. This model states that the backscattered signal results as the product between a Gaussian speckle noise vector component and a random scalar texture component. Hence, the assumption is that the texture has the same statistical distribution and is fully correlated in all polarimetric channels. This assumption has to some extent been disputed due to the fact that in e.g. scattering from forested areas, volume scattering will effect the cross-polarization component stronger than the co-polarization channels, whereas surface scattering will have the opposite effect. The volume and surface scattering mechanisms may have different texture properties because of their physically distinct origins.

In this paper we examine an extended multivariate product model, in which each polarimetric channel may be characterized by an individual random texture variable. Let the scattering vector be given as $\mathbf{s} = [S_{hh}\, S_{hv}\, S_{vh}\, S_{vv}]^T$, where the indices refer to the transmit and receive polarization, respectively. In the multitexture statistical model we have

$$\mathbf{s} = \mathbf{T}^{1/2}\mathbf{x} \tag{1}$$

where $\mathbf{T} = \mathrm{diag}\{T_{hh}, T_{hv}, T_{vh}, T_{vv}\}$ is a diagonal matrix containing the texture variables associated with the respective polarimetric channels, and $\mathbf{x}$ is a zero mean, circular complex Gaussian vector variable, representing speckle [3]. Hence, the covariance of $\mathbf{s}$, conditioned on the texture matrix $\mathbf{T}$, is

$$\mathbf{\Sigma_s}|\mathbf{T} = \mathbf{T}^{1/2}\mathbf{\Sigma_x}\mathbf{T}^{1/2} \tag{2}$$

with $\mathbf{\Sigma_x}$ being the covariance of $\mathbf{x}$. It is well-known that the probability density function (pdf) of the sample covariance matrix for a Gaussian vector follows the scaled Wishart distribution [4]. Let the sample covariance of $\mathbf{x}$ be given by

$$\mathbf{W} = \frac{1}{L}\sum_{i=1}^{L}\mathbf{x}_i\mathbf{x}_i^H \tag{3}$$

where $(\cdot)^H$ denotes Hermitian transpose. Its pdf becomes

$$f_{\mathbf{W}}(\mathbf{W}; L, \mathbf{\Sigma_x}) = \frac{L^{Ld}}{\Gamma_d(L)}\frac{|\mathbf{W}|^{L-d}}{|\mathbf{\Sigma_x}|^L}\,\mathrm{etr}(-L\mathbf{\Sigma_x}^{-1}\mathbf{W}) \tag{4}$$

where $d = 4$, $|\cdot|$ is a determinant, $\mathrm{etr}(\cdot)$ is the exponential trace operator, and $\Gamma_d(L)$ is the multivariate gamma function of the complex kind. Furthermore, if texture can be assumed constant on the scale of the multilook window, the sample covariance matrix of $\mathbf{s}$ becomes

$$\mathbf{C} = \frac{1}{L}\sum_{i=1}^{L}\mathbf{s}_i\mathbf{s}_i^H = \mathbf{T}^{1/2}\mathbf{W}\mathbf{T}^{1/2}\,. \tag{5}$$

Hence, the pdf of $\mathbf{C}$, given $\mathbf{T}$, is readily obtained from (4) as

$$\begin{aligned} &f_{\mathbf{C}|\mathbf{T}}(\mathbf{C}|\mathbf{T}; L, \mathbf{\Sigma_x}) \\ &\quad = f_{\mathbf{W}}(\mathbf{T}^{-1/2}\mathbf{C}\mathbf{T}^{-1/2}; L, \mathbf{\Sigma_x})\cdot|J_{\mathbf{W}\to\mathbf{C}}| \\ &\quad = \frac{L^{Ld}}{\Gamma_d(L)}\frac{|\mathbf{C}|^{L-d}}{|\mathbf{T}|^L|\mathbf{\Sigma_x}|^L}\,\mathrm{etr}(-L\mathbf{\Sigma_x}^{-1}\mathbf{T}^{-1/2}\mathbf{C}\mathbf{T}^{-1/2}) \end{aligned} \tag{6}$$

where $J_{\mathbf{W}\to\mathbf{C}}$ is the Jacobian of the transformation from $\mathbf{W}$ to $\mathbf{C}$. The marginal distribution for $\mathbf{C}$ is obtained by integrating over the pdf of $\mathbf{T}$, i.e.

$$f_{\mathbf{C}}(\mathbf{C}; L, \mathbf{\Sigma_x}) = \int f_{\mathbf{C}|\mathbf{T}}(\mathbf{C}|\mathbf{T}; L, \mathbf{\Sigma_x}) f_{\mathbf{T}}(\mathbf{T})d\mathbf{T}\,. \tag{7}$$

We will here present both theoretical and practical aspects associated with of above described model, and discuss its significances in the analysis of multipolarimetric SAR data.

2. MULTITEXTURE PDF UNDER RECIPROCITY AND REFLECTION SYMMETRY

The four-by-four covariance matrix describes the polarimetric backscattering properties of all kinds of targets. For reciprocal media the relation $S_{hv} = S_{vh}$ reduces the covariance matrix to a three-by-three matrix of the form

$$\boldsymbol{\Sigma}_{\mathbf{s}} = \begin{pmatrix} \sigma_{hhhh} & \sqrt{2}\sigma_{hhhv} & \sigma_{hhvv} \\ \sqrt{2}\sigma^*_{hhhv} & 2\sigma_{hvhv} & \sqrt{2}\sigma_{hvvv} \\ \sigma^*_{hhvv} & \sqrt{2}\sigma^*_{hvvv} & \sigma_{vvvv} \end{pmatrix} \tag{8}$$

where the factor $\sqrt{2}$ secures matrix span invariance. Hence, the multitexture is represented by a three-by-three diagonal matrix, with $\mathbf{T} = \mathrm{diag}\{T_{hh}, T_{hv}, T_{vv}\}$. If we assume reflection symmetry, then (8) simplifies to

$$\boldsymbol{\Sigma}_{\mathbf{s}} = \begin{pmatrix} \sigma_{hhhh} & 0 & \sigma_{hhvv} \\ 0 & 2\sigma_{hvhv} & 0 \\ \sigma^*_{hhvv} & 0 & \sigma_{vvvv} \end{pmatrix} \tag{9}$$

where it is noted that $\boldsymbol{\Sigma}_{\mathbf{s}} = \mathrm{E}_{\mathbf{T}}\{\mathbf{T}^{\frac{1}{2}}\boldsymbol{\Sigma}_{\mathbf{x}}\mathbf{T}^{\frac{1}{2}}\}$, where $\mathrm{E}_{\mathbf{T}}\{\cdot\}$ denotes expectation with regard to the texture matrix variable $\mathbf{T}$, and $\boldsymbol{\Sigma}_{\mathbf{x}}$ has the same structure as $\boldsymbol{\Sigma}_{\mathbf{s}}$. The inverse matrix $\boldsymbol{\Sigma}_{\mathbf{x}}^{-1}$ will have the same zero elements as $\boldsymbol{\Sigma}_{\mathbf{x}}$. Let $q_{i,j}$ and $c_{i,j}$ denote entry (i,j) of $\boldsymbol{\Sigma}_{\mathbf{x}}^{-1}$ and the sample covariance matrix $\mathbf{C}$, respectively. Eq. (6) then takes the form

$$\begin{aligned} f_{\mathbf{C}|\mathbf{T}}(\mathbf{C}|\mathbf{T}; L, \boldsymbol{\Sigma}_{\mathbf{x}}) &= \frac{L^{3L}}{\Gamma_3(L)} \frac{|\mathbf{C}|^{L-3}}{|\boldsymbol{\Sigma}_{\mathbf{x}}|^L} \frac{1}{T_{hh}T_{hv}T_{vv}} \\ &\times \exp\left\{-L\left(\frac{q_{11}c_{11}}{T_{hh}} + \frac{q_{13}c_{31}}{\sqrt{T_{hh}T_{vv}}} + \frac{q_{22}c_{22}}{T_{hv}}\right.\right. \\ &\left.\left. + \frac{q_{31}c_{13}}{\sqrt{T_{hh}T_{vv}}} + \frac{q_{33}c_{33}}{T_{vv}}\right)\right\} \end{aligned} \tag{10}$$

We further make the assumption that the texture components T_{hh} and T_{vv} are equal. Then the distribution of the sample covariance matrix $\mathbf{C}$ under the assumption of monostatic radar geometry, reciprocity and reflection symmetry becomes

$$\begin{aligned} f_{\mathbf{C}}(\mathbf{C}; L, \boldsymbol{\Sigma}_{\mathbf{x}}, \boldsymbol{\theta}) &= \frac{L^{3L}}{\Gamma_3(L)} \frac{|\mathbf{C}|^{L-3}}{|\boldsymbol{\Sigma}_{\mathbf{x}}|^L} \\ &\times \int \exp\left\{-L\left(\frac{q_{11}c_{11} + q_{13}c_{31} + q_{31}c_{13} + q_{33}c_{33}}{T_{hh}}\right)\right\} \\ &\quad \times \frac{f_{T_{hh}}(T_{hh}; \boldsymbol{\theta}_{hh})}{T_{hh}^{2L}}\, dT_{hh} \\ &\times \int \exp\left\{-L\left(\frac{q_{22}c_{22}}{T_{hv}}\right)\right\} \frac{f_{T_{hv}}(T_{hv}; \boldsymbol{\theta}_{hv})}{T_{hv}^{L}}\, dT_{hv} \end{aligned} \tag{11}$$

where $f_{T_{hh}}(T_{hh}; \boldsymbol{\theta}_{hh})$ and $f_{T_{hv}}(T_{hv}; \boldsymbol{\theta}_{hv})$ denote the pdfs of T_{hh} and T_{hv}, with respective texture parameter vectors, $\boldsymbol{\theta}_{hh}$ and $\boldsymbol{\theta}_{hv}$, gathered in $\boldsymbol{\theta} = [\boldsymbol{\theta}_{hh}^T; \boldsymbol{\theta}_{hv}^T]^T$. The model proposed in Eq. (11) gives the freedom to assume different texture distributions for the co- and cross-polarimetric channels. The integrals can be evaluated in closed form for all recently introduced texture models like the gamma, inverse gamma, inverse Gaussian, and Fisher distributions, to name a few.

3. MELLIN KIND STATISTICS

The Mellin kind statistics (MKS) of the multitexture product model are derived in this section. MKS is a theoretical framework for statistical analysis of single polarization amplitude and intensity radar data proposed by Nicolas [5] and extended to multilook polarimetric radar data in [4].

Recall the multitexture model from (5) as $\mathbf{C} = \mathbf{T}^{\frac{1}{2}}\mathbf{W}\mathbf{T}^{\frac{1}{2}}$. The Mellin kind characteristic function (cf) of $\mathbf{C}$ is defined as the matrix-variate Mellin transform of $f_{\mathbf{C}}(\mathbf{C})$: $\phi_{\mathbf{C}}(s) = \mathcal{M}\{f_{\mathbf{C}}(\mathbf{C})\}(s) = \mathrm{E}\{|\mathbf{C}|^{s-d}\}$ [4]. For the matrix product above, it is known that the Mellin kind cf becomes [4]

$$\phi_{\mathbf{C}}(s) = \phi_{\mathbf{T}}(s) \cdot \phi_{\mathbf{W}}(s) \tag{12}$$

which shows that the Mellin kind cf decomposes into a product of the texture and the speckle contribution. The contribution of the scaled Wishart matrix, $\mathbf{W}$, was derived in [4] as

$$\phi_{\mathbf{W}}(s) = \frac{\Gamma_d(L+s-d)}{\Gamma_d(L)} \left(\frac{|\boldsymbol{\Sigma}|}{L^d}\right)^{s-d} \tag{13}$$

and can thus be removed to isolate the texture part. By definition, the Mellin kind cf of $\mathbf{T}$ is

$$\phi_{\mathbf{T}}(s) = \mathrm{E}\{|\mathbf{T}|^{s-d}\} \tag{14}$$

and since $\mathbf{T}$ is diagonal it follows that

$$\phi_{\mathbf{T}}(s) = \mathrm{E}\left\{\prod_{i=1}^{d} T_i^{s-d}\right\}. \tag{15}$$

This is the general case, before any assumptions have been made about the correlation between the texture variables.

Let the matrix log-moment (MLM) or order ν be defined as the logarithmic moment of the matrix determinant:

$$\mu_\nu\{\mathbf{C}\} = \mathrm{E}\{(\log|\mathbf{C}|)^\nu\}. \tag{16}$$

Matrix log-cumulants (MLC) of order ν, denoted $\kappa_\nu\{\mathbf{C}\}$, are then defined through the well-known relations between moments and cumulants [6, ch.3]:

$$\kappa_1 = \mu_1 \tag{17a}$$
$$\kappa_2 = \mu_2 - \mu_1^2 \tag{17b}$$
$$\kappa_3 = \mu_3 - 3\mu_2\mu_1 + 2\mu_1^3 \tag{17c}$$
$$\kappa_4 = \mu_4 - 4\mu_3\mu_1 - 3\mu_2^2 + 12\mu_2\mu_1^2 - 6\mu_1^4 \tag{17d}$$

The reference to the matrix $\mathbf{C}$ is dropped in the above equations since the relations are general and valid for moments and cumulants of all sorts of random variates. The sample MLMs of order ν are computed from

$$\langle\mu_\nu\{\mathbf{C}\}\rangle = \frac{1}{n}\sum_{i=1}^{n}(\log|\mathbf{C}|)^\nu \tag{18}$$

and can be combined into unique symmetric unbiased estimators of the population MLCs, known as k-statistics and denoted $\langle \kappa_\nu\{\mathbf{C}\}\rangle$, by relations given in [6, ch.12]. The population MLCs can be retrieved from the Mellin kind cf by

$$\kappa_\nu\{\mathbf{C}\} = \left.\frac{d^\nu}{ds^\nu}\log\phi_{\mathbf{C}}(s)\right|_{s=d}. \tag{19}$$

In the following, let $T_x \perp T_y$ denote that texture variables T_x and T_y are statistically independent, and let $T_x \parallel T_y$ denote that they are totally correlated, that is, identical. The hh and vv channels are referred to as the co-polarization (co-pol) channels and the hv and vh channels as the cross-polarization (cross-pol) channels. Further, let the complete set of polarimetric channels available be denoted by $\mathcal{P}$, the subset of co-pol channels by $\mathcal{P}_{co}$, and the subset of cross-pol channels by $\mathcal{P}_x$. The respective sizes of these sets are denoted d, d_{co}, and d_x. Now consider the Mellin kind cf under particular sets of assumptions.

Case (i): $T_{hh} \perp T_{hv} \perp T_{vh} \perp T_{vv}$ (all texture variables mutually independent). When the texture variables for all polarizations are statistically independent, (15) simplifies to

$$\phi_{\mathbf{T}}(s) = \prod_{i\in\mathcal{P}} \mathrm{E}\left\{T_i^{s-d}\right\} = \prod_{i\in\mathcal{P}} \phi_{T_i}(s-d+1) \tag{20}$$

where $\mathcal{P} = \{hh, hv, vh, vv\}$ and $d = 4$ when full-polarimetric data are recorded. The MLCs in this case evaluate to

$$\kappa_\nu\{\mathbf{C}\} = \kappa_\nu\{\mathbf{W}\} + \sum_{i\in\mathcal{P}} \kappa_\nu\{T_i\}. \tag{21}$$

Case (ii): $T_{hh} \parallel T_{vv}, T_{hv} \parallel T_{vh}, T_{hh} \perp T_{hv}, T_{vv} \perp T_{vh}$ (co-pol and cross-pol texture variables mutually independent; full correlation within co-pol and cross-pol texture variables). In this special case, the co-pol texture variables are identical, the cross-pol texture variables are identical, and the co-pol texture variable is totally decoupled from the cross-pol texture variable due to statistical independence. Therefore, the co-pol and cross-pol contributions to $\phi_{\mathbf{T}}(s)$ can be separated as a product.

$$\begin{aligned}\phi_{\mathbf{T}}(s) &= \mathrm{E}\left\{\prod_{i\in\mathcal{P}_{co}}^{d_{co}} T_i^{s-d_{co}}\right\}\mathrm{E}\left\{\prod_{i\in\mathcal{P}_x}^{d_x} T_i^{s-d_x}\right\}\\ &= \mathrm{E}\left\{T_{co}^{d_{co}(s-d_{co})}\right\}\mathrm{E}\left\{T_x^{d_x(s-d_x)}\right\}\\ &= \phi_{T_{co}}(d_{co}(s-d_{co})+1)\cdot\phi_{T_x}(d_x(s-d_x)+1)\end{aligned} \tag{22}$$

where the common co-pol texture variable and the common cross-pol texture variable variable are denoted T_{co} and T_x, respectively. This property translates to an additive decomposition of their MLCs.

$$\kappa_\nu\{\mathbf{C}\} = \kappa_\nu\{\mathbf{W}\} + d_{co}^\nu\,\kappa_\nu\{T_{co}\} + d_x^\nu\kappa_\nu\{T_x\} \tag{23}$$

Case (iii): $T_{hh} \parallel T_{hv} \parallel T_{vh} \parallel T_{vv}$ (all texture variables fully correlated). This case is equivalent to the scalar product model, where the texture variables are identical for all polarizations, denoted as T. The Mellin kind cf is known as [4]

$$\begin{aligned}\phi_{\mathbf{T}}(s) &= \mathrm{E}\left\{T^{d(s-d)}\right\}\\ &= \phi_{\mathbf{T}}\big(d(s-d)+1\big)\end{aligned} \tag{24}$$

and the MLCs

$$\kappa_\nu\{\mathbf{C}\} = \kappa_\nu\{\mathbf{W}\} + d^\nu\kappa_\nu\{T\}. \tag{25}$$

In order to compare the results obtained in the different special cases, it is useful to isolate $\kappa_\nu\{\mathbf{T}\}$. The texture variables are not directly observable, but their contribution to the MLCs can be measured by removing the theoretical speckle contribution through

$$\langle\kappa_\nu\{\mathbf{T}\}\rangle = \langle\kappa_\nu\{\mathbf{C}\}\rangle - \kappa_\nu\{\mathbf{W}\}. \tag{26}$$

The alternative models can be summarized as

$$\kappa_\nu\{\mathbf{T}\} = \begin{cases}\displaystyle\sum_{i=1}^{d}\kappa_\nu\{T_i\} & :\ \text{case (i)}\\ d_{co}^\nu\,\kappa_\nu\{T_{co}\} + d_x^\nu\kappa_\nu\{T_x\} & :\ \text{case (ii)}\\ d^\nu\kappa_\nu\{T\} & :\ \text{case (iii)}\end{cases} \tag{27}$$

The special cases discussed above only treat full correlation or statistical independence (no correlation) between the texture variables. In reality, it would be expected to find intermediate levels of correlation. It can be observed from (27) that the effect of correlation is to increase the degree of texture. Assume that all texture variable have the same distribution and then compare all cases. It is then seen that the MLC magnitude increases from case (i) through case (ii) to case (iii): $d|\kappa_\nu\{\mathbf{T}\}| < (d_{co}^\nu + d_x^\nu)|\kappa_\nu\{\mathbf{T}\}| < d^\nu|\kappa_\nu\{\mathbf{T}\}|$. This is intuitively correct, since the effect or correlation is to align the contribution of the correlated variables, such that their combined impact becomes more extreme.

4. RESULTS: HYPOTHESIS TESTING

The MKS framework provides tools suitable for selection of the appropriate texture model for a particular image data set. Specifically, the goodness-of-fit (GoF) testing described in [7] can be used to develop hypothesis tests based on log-cumulants of multiple orders, given the measured sample log-cumulants, the estimated model parameters, and the sample size. Fig. 1 illustrates how the testing proceeds.

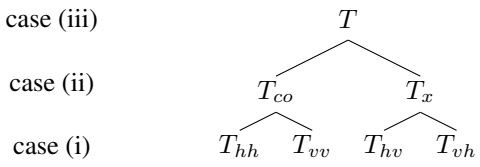

Fig. 1. Hypothesis test scheme

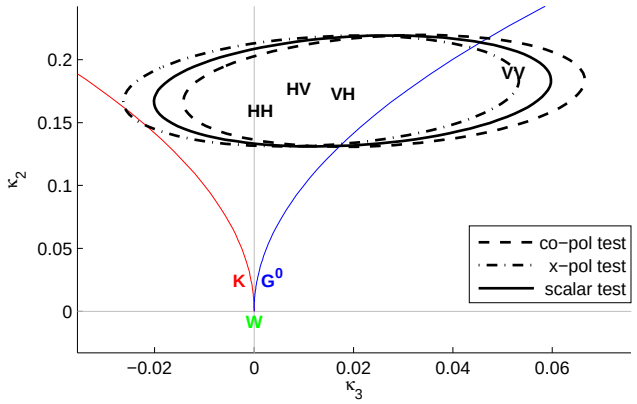

Fig. 2. Log-cumulant diagram with evidence of scalar texture for a forest segment in a PALSAR image from the Amazon.

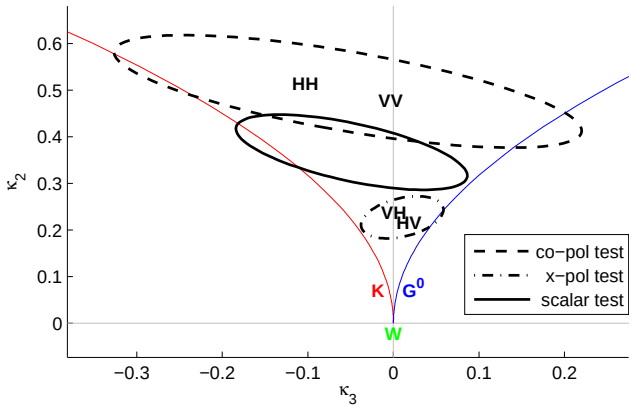

Fig. 3. Log-cumulant diagram with evidence of multitexture for a sea ice segment in a PALSAR image from Spitsbergen.

Three tests are sufficient to distinguish the three cases described in Section 3. First test all four channels combined for a common scalar texture variable, referred to as the scalar test. If the test passes, we have case (iii), the traditional scalar texture model. Otherwise, test both the co-pol channels for a common texture variable and the cross-pol channels for a common texture variable. If these tests pass, we have case (ii). Otherwise, we have case (i), with independent texture variables for all channels.

All tests are performed in the same fashion; To test if the texture variables associated with data partition A and B can be merged into a texture variable corresponding to the pooled data, $C = A \cup B$, we compute the second and third-order sample log-cumulants, κ_2 and κ_3, of all data partitions. Each texture variable is then associated with a point in the κ_3/κ_2-plane [4, 7], which is the space shown in Figs. 2 and 3. A χ^2-distributed GoF test statistic from [7] defines a distance measure in the κ_3/κ_2-plane, which we use to find the probability of the (κ_3, κ_2) values associated with A and B being realizations of a merged texture variable, characterized by the (κ_3, κ_2) value associated with C.

In Figs. 2 and 3, the symbols HH, HV, VH and VV show the (κ_3, κ_2) points for all polarimetric channels. The 95% confidence regions of the merged co-pol, cross-pol, and scalar test are determined from the sampling distribution of our test statistic [7]. These are shown as ellipses with dashed, dot-dashed, and solid lines, respectively. The red line, the blue line, and the green origin represent population log-cumulants of the K distribution [1], the G^0 distribution, and the complex Wishart distribution [2], respectively. Fig. 2 presents results for a forest sample, where all channels fall within the confidence region of the scalar test, indicating case (iii). Fig. 3 presents results for a sample of sea ice, where the co-pol and the cross-pol channels can be merged pairwise, but the test for merging of all channels fails, thereby selecting the multitexture model of case (ii).

5. CONCLUSIONS

A multitexture model for PolSAR data has been developed, including model density functions, log-cumulant expressions and hypothesis test validation. Preliminary results on several distinctly different PolSAR scenes indicate that the scalar product model is often valid, and otherwise the co-pol/cross-pol paired case (ii) is common. Care must be taken to avoid class boundaries when sampling images, as the theoretical framework is based upon pure classes and mixtures always result in exaggerated and often multiple textures.

6. REFERENCES

[1] A.-P. Doulgeris, S.N. Anfinsen, and T. Eltoft, "Classification with a non-Gaussian model for PolSAR data," *IEEE Trans. Geosci. Remote Sens.*, vol. 46, no. 10, pp. 2999–3009, Oct. 2008.

[2] C.C. Freitas, A.C. Frery, and A.H. Correia, "The polarimetric G distribution for SAR data analysis," *Environmetrics*, vol. 16, no. 1, pp. 13–31, Feb. 2005.

[3] Y. Yu, "Textural-partially correlated polarimetric K-distribution," in *Proc. IEEE Int. Geosci. Remote Sens. Symp., IGARSS'98*, Seattle, USA, 6-10 July 1998, vol. 4, pp. 2098–2100.

[4] S.N. Anfinsen and T. Eltoft, "Application of the matrix-variate Mellin transform to analysis of polarimetric radar images," *IEEE Trans. Geosci. Remote Sens.*, vol. 49, no. 7, pp. 2281–2295, June 2011.

[5] J.-M. Nicolas, "Introduction aux statistique de deuxième espèce: Application des logs-moments et des logs-cumulants à l'analyse des lois d'images radar," *Traitement du Signal*, vol. 19, no. 3, pp. 139–167, 2002.

[6] A. Stuart and J.K. Ord, *Kendall's Advanced Theory of Statistics: Distribution Theory*, vol. 1, Edward Arnold, London, UK, sixth edition, 1994.

[7] S.N. Anfinsen, A.P. Doulgeris, and T. Eltoft, "Goodness-of-fit tests for multilook polarimetric radar data based on the Mellin transform," *IEEE Trans. Geosci. Remote Sens.*, vol. 49, no. 8, July 2011, 2764–2781.